International Journal of Heat and Mass Transfer 55 (2012) 384–394

Contents lists available at SciVerse ScienceDirect

International Journal of Heat and Mass Transfer

journal homepage: www.elsevier.com/locate/ijhmt

Local thermal non-equilibrium effects in the Darcy–Bénard instability with isoflux boundary conditions

A. Barletta [a,*], D.A.S. Rees [b]

[a] DIENCA, Alma Mater Studiorum – Università di Bologna, Viale Risorgimento 2, Bologna 40136, Italy
[b] Department of Mechanical Engineering, University of Bath, Claverton Down, Bath BA2 7AY, UK

ARTICLE INFO

Article history:
Received 30 April 2011
Received in revised form 31 August 2011
Available online 11 October 2011

Keywords:
Porous medium
Darcy–Bénard problem
Buoyancy-induced instability
Local thermal non-equilibrium
Constant heat flux

ABSTRACT

The Darcy–Bénard problem with constant heat flux boundary conditions is studied in a regime where the fluid and solid phases are in local thermal non-equilibrium. The onset conditions for convective instability in the plane porous layer are investigated using a linear stability analysis. Constant heat flux boundary conditions are formulated according to the Amiri–Vafai–Kuzay Model A, where the boundary walls are assumed as impermeable and with a high thermal conductance. The normal mode analysis of the perturbations imposed on the basic state leads to a one-dimensional eigenvalue problem, solved numerically to determine the neutral stability condition. Analytical solutions are found for the limit of small wave numbers, and in the regime where the conductivity of the solid phase is much larger than the conductivity of the fluid phase. A comparison with the corresponding results under conditions of local thermal equilibrium is carried out. The critical conditions for the onset of convection correspond to a zero wave number only when the inter-phase heat transfer coefficient is sufficiently large. Otherwise, the critical conditions correspond to a nonzero wave number.

1. Introduction

The onset of convection in porous media due to an externally imposed thermal gradient, originally formulated and solved in the pioneering papers by Horton and Rogers [1] and by Lapwood [2], is now a classical topic in fluid dynamics. The original statement of this problem, well-known as Darcy–Bénard problem or as the Horton–Rogers–Lapwood problem, corresponds to a plane porous channel bounded by a pair of isothermal walls kept at different temperatures. Among the many developments of these papers, reviewed extensively in Chapter 6 of Nield and Bejan [3], here we focus our attention on the analysis of the thermoconvective instability in a fluid saturated porous medium under conditions of local thermal non-equilibrium.

Local thermal non-equilibrium in a porous medium saturated by a fluid is modelled by assuming two temperature fields, one for the solid phase and one for the fluid phase. An inter-phase heat transfer coefficient h is defined, so that the local energy balance equations for the fluid phase and for the solid phase contain heat exchange terms proportional to h and to the local temperature difference between the phases. This model, formulated following the earlier studies by Anzelius [4] and Schumann [5], and by other investigators such as Combarnous and Bories [6], is nowadays established in the form expressed by Nield and Bejan [3]. Surveys of the main results obtained on applying this non-equilibrium model to the analysis of convection in porous media have been carried out by Kuznetsov [7] and by Rees and Pop [8].

The two-temperature model was first employed in a linear stability analysis of the Darcy–Bénard problem by Banu and Rees [9]. This study, which is based on Darcy's law, uses the same boundary conditions as those considered by Horton and Rogers [1] and by Lapwood [2], namely constant temperature conditions. An extension of the analysis by Banu and Rees [9] to a more general local momentum balance equation, including both the form-drag term and the Brinkman term, was carried out by Postelnicu and Rees [10] for the case of stress-free isothermal boundaries, and by Postelnicu [11] for the case of isothermal rigid boundaries. Malashetty et al. [12] investigated the onset of the thermoconvective instability in the case of a non-isotropic porous medium under local non-equilibrium conditions. Heat generation occurring either in the fluid phase or in the solid phase has been taken into account by Nouri-Borujerdi et al. [13], together with the temperature difference between the boundary walls, as the possible source of the thermal instability in a horizontal porous layer. All these papers deal with extensions of the Darcy–Bénard problem under the hypothesis of local thermal non-equilibrium, assuming thermal boundary conditions of the Dirichlet type. The case of Neumann thermal boundary conditions, i.e. uniform heat flux, have not been considered thus far and form the objective of the present study.

* Corresponding author.
E-mail address: antonio.barletta@unibo.it (A. Barletta).

0017-9310/$ - see front matter © 2011 Elsevier Ltd. All rights reserved.
doi:10.1016/j.ijheatmasstransfer.2011.09.031

Nomenclature

a	dimensionless wave number
A; B	integration constants
c	heat capacity per unit mass
$\mathbf{e}_z$	unit vector in the z-direction
$\mathbf{g}$; g	gravitational acceleration; modulus of $\mathbf{g}$
h	inter-phase heat transfer coefficient
H	dimensionless inter-phase heat transfer parameter, Eq. (8)
k	thermal conductivity
K	permeability
L	layer thickness
n	natural number
q_w	wall heat flux
R	Darcy–Rayleigh number, Eq. (8)
$\widehat{R}$	modified Darcy–Rayleigh number, Eq. (64)
t	dimensionless time, Eq. (6)
T	dimensionless temperature, Eq. (6)
$\mathbf{u}$	dimensionless velocity, (u,v,w), Eq. (6)
$\mathbf{U}$	dimensionless velocity disturbance, (U,V,W), Eq. (15)
$\mathbf{x}$	dimensionless position vector, (x,y,z), Eq. (6)

Greek symbols

α	thermal diffusivity
β	thermal expansion coefficient
γ	dimensionless parameter, Eq. (8)
ΔT	reference temperature difference, Eq. (7)
ε	dimensionless perturbation parameter, Eq. (15)
Θ	dimensionless fluid phase temperature disturbance, Eq. (15)
$\widetilde{\Theta}, \widetilde{\Phi}, \widetilde{\Psi}$	dimensionless disturbance amplitudes, Eq. (26)
$\widetilde{\Theta}_n, \widetilde{\Phi}_n, \widetilde{\Psi}_n, R_n$	power series coefficients, Eq. (43)
λ	dimensionless parameter, Eq. (8)
$\widetilde{\Lambda}$	dimensionless function, Eq. (31)
μ	dynamic viscosity
ν	kinematic viscosity
ρ	density
φ	porosity
Φ	dimensionless solid phase temperature disturbance, Eq. (15)
Ψ	dimensionless streamfunction disturbance, Eq. (21)
ζ	equal to $z-\frac{1}{2}$
σ	equal to $\sqrt{H(\gamma+1)}$

Superscript, subscripts

–	dimensional quantity
B	basic solution
c	critical value
f	fluid phase
m	volumetric average over the phases
s	solid phase
th	threshold value
′	differentiation with respect to z

This paper provides a linear stability analysis for a horizontal porous layer with a uniform heat flux prescribed on the plane boundary walls. The regime of local thermal non-equilibrium is studied including, as special cases, the limits of zero and infinite inter-phase heat transfer coefficient. The former limit is the regime of thermally decoupled phases, where the temperature field of the fluid is independent of the temperature field of the solid. The latter limit corresponds to local thermal equilibrium, investigated originally by Nield [14] and described in detail in Section 6.2 of Nield and Bejan [3]. We also investigate the two limits where the thermal conductivity of the fluid phase is either much larger or much smaller than the thermal conductivity of the solid phase. In the latter case, the linear stability problem admits a completely analytical solution.

2. Problem statement and governing equations

We consider a plane porous layer having thickness L, bounded at $\bar{z}=0$ and at $\bar{z}=L$ by impermeable boundaries where a uniform heat flux, q_w, is prescribed (see Fig. 1). The buoyant flow in the porous layer is studied under the following assumptions:

- The porous medium is homogeneous and isotropic;
- The Oberbeck–Boussinesq approximation holds;
- Darcy's law holds;
- The viscous dissipation effect is negligible and volumetric heating is absent;
- The local thermal non-equilibrium between the solid and fluid phases is modeled through an inter-phase heat transfer coefficient h.

2.1. Governing equations

As a consequence of the basic assumptions, the governing local balance equations can be written as

$$\bar{\nabla}\cdot\bar{\mathbf{u}}=0, \tag{1}$$

$$\frac{\mu}{K}\bar{\nabla}\times\bar{\mathbf{u}}=\rho_f g\beta\bar{\nabla}\times(\overline{T}_f\mathbf{e}_z), \tag{2}$$

$$(1-\varphi)(\rho c)_s\frac{\partial\overline{T}_s}{\partial\bar{t}}=(1-\varphi)k_s\bar{\nabla}^2\overline{T}_s+h(\overline{T}_f-\overline{T}_s), \tag{3}$$

$$\varphi(\rho c)_f\frac{\partial\overline{T}_f}{\partial\bar{t}}+(\rho c)_f\bar{\mathbf{u}}\cdot\bar{\nabla}\overline{T}_f=\varphi k_f\bar{\nabla}^2\overline{T}_f+h(\overline{T}_s-\overline{T}_f). \tag{4}$$

Eq. (2) represents the vorticity formulation of Darcy's law. In fact, the curl operator has been applied to the local momentum balance equation in order to eliminate the pressure field.

2.2. Boundary conditions

The boundary conditions for the seepage velocity, $\bar{\mathbf{u}}=(\bar{u},\bar{v},\bar{w})$, and for the temperature fields, $\overline{T}_f,\overline{T}_s$, may be expressed according to the models formulated by Amiri et al. [15] and recently revisited by Yang and Vafai [16].

In the present study, we will adopt the so-called Model A [16].

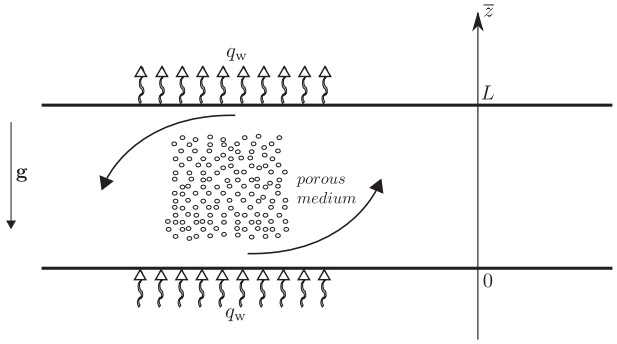

Fig. 1. Schematic of the porous layer.

This model of the constant heat flux boundary conditions is based on the assumption that the boundaries $\bar{z} = 0, L$ are in a condition of local thermal equilibrium. Moreover, it is assumed that the supplied wall heat flux q_w is given by the sum of the Fourier heat fluxes

$$-k_f \frac{\partial \overline{T}_f}{\partial \bar{z}}, \quad -k_s \frac{\partial \overline{T}_s}{\partial \bar{z}},$$

in the fluid phase and in the solid phase, where each flux is weighted by the volumetric fraction of the corresponding phase, φ and $1-\varphi$ respectively. Thus, the velocity and temperature boundary conditions can be written as

$$\bar{z} = 0, L : \begin{cases} \bar{w} = 0, \\ -\varphi k_f \dfrac{\partial \overline{T}_f}{\partial \bar{z}} - (1-\varphi) k_s \dfrac{\partial \overline{T}_s}{\partial \bar{z}} = q_w, \\ \overline{T}_f = \overline{T}_s. \end{cases} \tag{5}$$

As pointed out by Yang and Vafai [16], this formulation of the constant heat flux boundary conditions is appropriate when the impermeable boundary wall is of finite thickness and with a high thermal conductivity. We mention that, in Eq. (5), the condition involving the heat fluxes is based on an energy balance at the boundary. There, the surface porosity is considered equal to the porosity φ. In fact, the latter assumption is legitimate for a homogeneous porous medium [17,18].

2.3. Dimensionless quantities

We define dimensionless variables as follows:

$$\bar{\mathbf{x}} = \mathbf{x} L, \quad \bar{t} = t \frac{L^2}{\alpha_f}, \quad \bar{\mathbf{u}} = \mathbf{u} \frac{\alpha_f}{L}, \quad \overline{T}_{s,f} = T_{s,f} \Delta T, \tag{6}$$

where

$$\Delta T = \frac{q_w L}{k_m}, \quad k_m = (1-\varphi) k_s + \varphi k_f. \tag{7}$$

We also introduce the dimensionless parameters

$$\lambda = \frac{\alpha_f}{\alpha_s}, \quad H = \frac{h L^2}{\varphi k_f}, \quad \gamma = \frac{\varphi k_f}{(1-\varphi) k_s}, \quad R = \frac{g \beta \Delta T K L}{\alpha_m \nu}. \tag{8}$$

Here, R is the Darcy–Rayleigh number. On the other hand, $\alpha_f = k_f/(\rho c)_f$ and $\alpha_s = k_s/(\rho c)_s$ are the thermal diffusivities of the fluid phase and of the solid phase respectively, while $\alpha_m = k_m/(\rho c)_f$ is the effective thermal diffusivity. Moreover, the kinematic viscosity is given by $\nu = \mu/\rho_f$. Then, Eqs. (1)–(4) may be rewritten in the form,

$$\nabla \cdot \mathbf{u} = 0, \tag{9}$$

$$\nabla \times \mathbf{u} = \varphi \frac{1+\gamma}{\gamma} R \nabla \times (T_f \mathbf{e}_z), \tag{10}$$

$$\lambda \frac{\partial T_s}{\partial t} = \nabla^2 T_s + H \gamma (T_f - T_s), \tag{11}$$

$$\frac{\partial T_f}{\partial t} + \frac{1}{\varphi} \mathbf{u} \cdot \nabla T_f = \nabla^2 T_f + H (T_s - T_f). \tag{12}$$

while the boundary conditions, Eq. (5), can be expressed as

$$z = 0, 1 : \begin{cases} w = 0, \\ -\gamma \dfrac{\partial T_f}{\partial z} - \dfrac{\partial T_s}{\partial z} = 1 + \gamma, \\ T_f = T_s. \end{cases} \tag{13}$$

We mention that, due to the constant heat flux boundary conditions, the solution of Eqs. (9)–(13) determines the temperature fields T_f and T_s only up to an arbitrary additive constant.

3. The basic solution

A steady-state solution of Eqs. (9)–(13) with a zero velocity exists,

$$\begin{cases} \mathbf{u}_B = 0, \\ T_{sB} = T_{fB} = 1 - z, \end{cases} \tag{14}$$

where "B" stands for basic solution. For all values of H, γ and λ the basic state solution is local thermal equilibrium basic solution. We have chosen the arbitrary additive constant in the expressions of T_{sB} and T_{fB} so that $T_{fB} = 0$ at $z = 1$.

4. Linear stability

We now perturb the basic solution,

$$\mathbf{u} = \mathbf{u}_B + \varepsilon \mathbf{U}, \quad T_s = T_{sB} + \varepsilon \Phi, \quad T_f = T_{fB} + \varepsilon \Theta, \tag{15}$$

where ε is a small perturbation parameter satisfying $|\varepsilon| \ll 1$. We substitute Eq. (15) into Eqs. (9)–(12) and neglect terms of $O(\varepsilon^2)$. Thus, we obtain the following linearized system,

$$\nabla \cdot \mathbf{U} = 0, \tag{16}$$

$$\nabla \times \mathbf{U} = \varphi \frac{1+\gamma}{\gamma} R \nabla \times (\Theta \mathbf{e}_z), \tag{17}$$

$$\lambda \frac{\partial \Phi}{\partial t} = \nabla^2 \Phi + H \gamma (\Theta - \Phi), \tag{18}$$

$$\frac{\partial \Theta}{\partial t} - \frac{1}{\varphi} W = \nabla^2 \Theta + H (\Phi - \Theta). \tag{19}$$

The linear stability analysis, carried out from Eqs. (16)–(19), is devoted to the determination of the onset conditions for the convective flow. The question of whether the bifurcation to convection is subcritical or supercritical will require the use of a weakly nonlinear theory involving terms up to $O(\varepsilon^3)$ in the local balance equations. Should the bifurcation be subcritical, then the energy method may be used to determine the depth of subcriticality where the solutions are then expected to be quite strongly nonlinear. As is well known, the nonlinearity becomes important in the evaluation of the rate of heat transfer, but this is outside of the scope of the present paper. This study is devoted entirely to the linear system, Eqs. (16)–(19), with the objective of determining the neutral stability conditions.

Given that the porous layer, the basic solution and the boundary conditions share a rotational symmetry about the z-axis, we conclude that the wave vector of the linear disturbances may be equivalently orientated in any direction within the horizontal (x,y)-plane. As a consequence it is not restrictive to assume two-dimensional disturbances lying in the (x,z)-plane. This means that we may write,

$$\begin{aligned} &U = U(x,z,t), \quad V = 0, \quad W = W(x,z,t), \\ &\Phi = \Phi(x,z,t), \quad \Theta = \Theta(x,z,t). \end{aligned} \tag{20}$$

Hence, Eq. (16) can be identically satisfied by defining a stream-function, $\Psi(x,z,t)$, such that

$$U = \varphi \frac{\partial \Psi}{\partial z}, \quad W = -\varphi \frac{\partial \Psi}{\partial x}. \tag{21}$$

On account of Eq. (21), Eqs. (17)–(19), yield

$$\nabla^2 \Psi + \frac{1+\gamma}{\gamma} R \frac{\partial \Theta}{\partial x} = 0, \tag{22}$$

$$\lambda \frac{\partial \Phi}{\partial t} = \nabla^2 \Phi + H \gamma (\Theta - \Phi), \tag{23}$$

$$\frac{\partial \Theta}{\partial t} + \frac{\partial \Psi}{\partial x} = \nabla^2 \Theta + H (\Phi - \Theta). \tag{24}$$

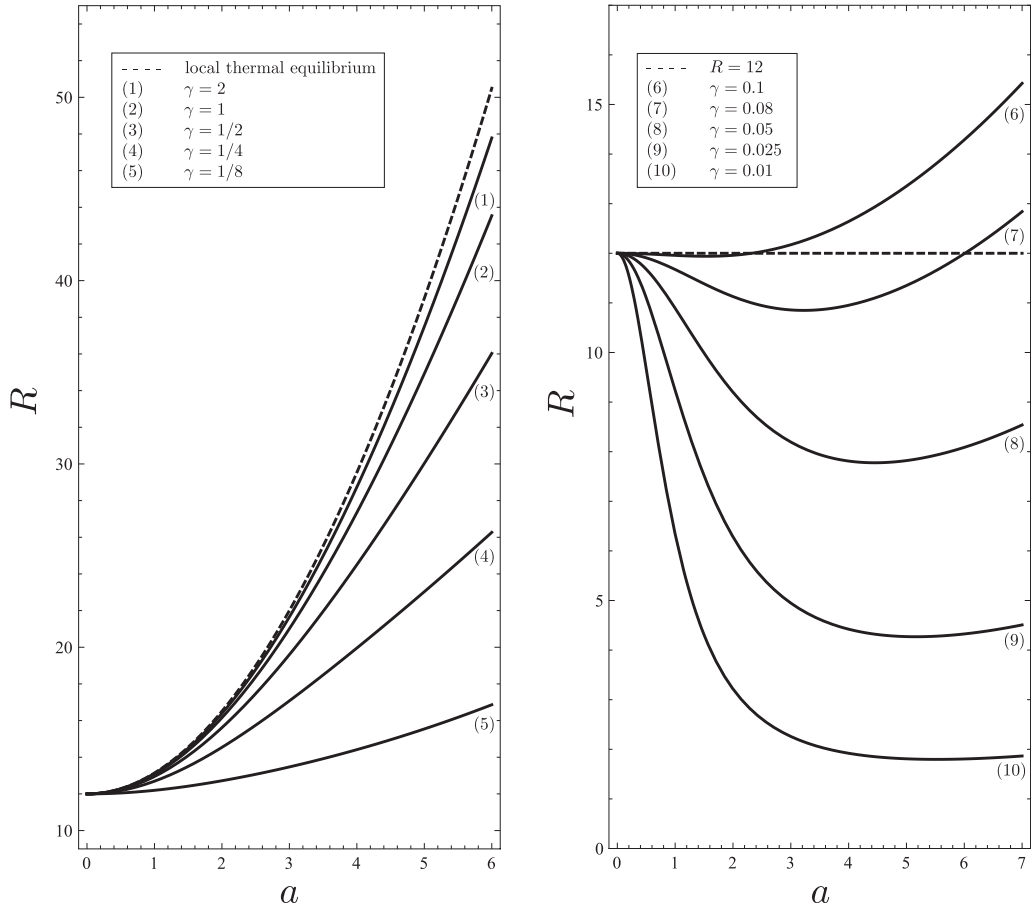

Fig. 2. Neutral stability curves for $H = 100$.

The boundary conditions associated with the eigenvalue problem Eqs. (22)–(24) are now given by

$$z = 0, 1 : \begin{cases} \Psi = 0, \\ \gamma \dfrac{\partial \Theta}{\partial z} + \dfrac{\partial \Phi}{\partial z} = 0, \\ \Theta = \Phi. \end{cases} \tag{25}$$

4.1. Stationary modes

It is possible to show using an integral method that solutions of Eqs. (22)–(25) either decay or grow exponentially in time and that the exponential growth rate is real. In other words, the principle of the exchange of stabilities applies, and therefore all modes of instability are stationary. Therefore we are able to set all time derivatives to zero in order to determine the onset criterion. We begin by substituting,

$$\Psi = \widetilde{\Psi}(z)\cos(ax), \quad \Phi = \widetilde{\Phi}(z)\sin(ax), \quad \Theta = \widetilde{\Theta}(z)\sin(ax). \tag{26}$$

into Eqs. (22)–(25) after which we obtain,

$$\widetilde{\Psi}'' - a^2\widetilde{\Psi} + a\frac{1+\gamma}{\gamma}R\widetilde{\Theta} = 0, \tag{27}$$

$$\widetilde{\Phi}'' - a^2\widetilde{\Phi} + H\gamma(\widetilde{\Theta} - \widetilde{\Phi}) = 0, \tag{28}$$

$$\widetilde{\Theta}'' - a^2\widetilde{\Theta} + H(\widetilde{\Phi} - \widetilde{\Theta}) + a\widetilde{\Psi} = 0, \tag{29}$$

$$z = 0, 1 : \widetilde{\Psi} = 0, \quad \gamma\widetilde{\Theta}' + \widetilde{\Phi}' = 0, \quad \widetilde{\Theta} = \widetilde{\Phi}, \tag{30}$$

where the primes denote differentiation with respect to z.

An alternative formulation of the differential problem Eqs. (27)–(30) may be obtained by defining the new dependent variable,

$$\widetilde{\Lambda}(z) = \widetilde{\Theta}(z) + \frac{\widetilde{\Phi}(z)}{\gamma}. \tag{31}$$

Thus, combination of Eqs. (28) and (29) allows one to rewrite Eqs. (27)–(30) as

$$\widetilde{\Psi}'' - a^2\widetilde{\Psi} + a\frac{1+\gamma}{\gamma}R\left(\widetilde{\Lambda} - \frac{\widetilde{\Phi}}{\gamma}\right) = 0, \tag{32}$$

$$\widetilde{\Lambda}'' - a^2\widetilde{\Lambda} + a\widetilde{\Psi} = 0, \tag{33}$$

$$\widetilde{\Phi}'' - a^2\widetilde{\Phi} + H\gamma\left(\widetilde{\Lambda} - \frac{1+\gamma}{\gamma}\widetilde{\Phi}\right) = 0, \tag{34}$$

$$z = 0, 1 : \widetilde{\Psi} = 0, \quad \widetilde{\Lambda}' = 0, \quad \widetilde{\Phi} = \frac{\gamma}{1+\gamma}\widetilde{\Lambda}. \tag{35}$$

4.1.1. The limit of local thermal equilibrium

Local thermal equilibrium occurs when the inter-phase heat transfer coefficient h becomes asymptotically large, i.e. in the limit $H \to \infty$. Within this regime, Eq. (28) can be satisfied only if $\widetilde{\Theta}(z) = \widetilde{\Phi}(z)$, for all z. Equivalently, if $H \to \infty$, Eq. (34) can be satisfied only if

$$\widetilde{\Lambda}(z) = \frac{1+\gamma}{\gamma}\widetilde{\Phi}(z), \tag{36}$$

for every z. Thus, in the limit of local thermal equilibrium the eigenvalue problem Eqs. (32)–(35) simplifies to

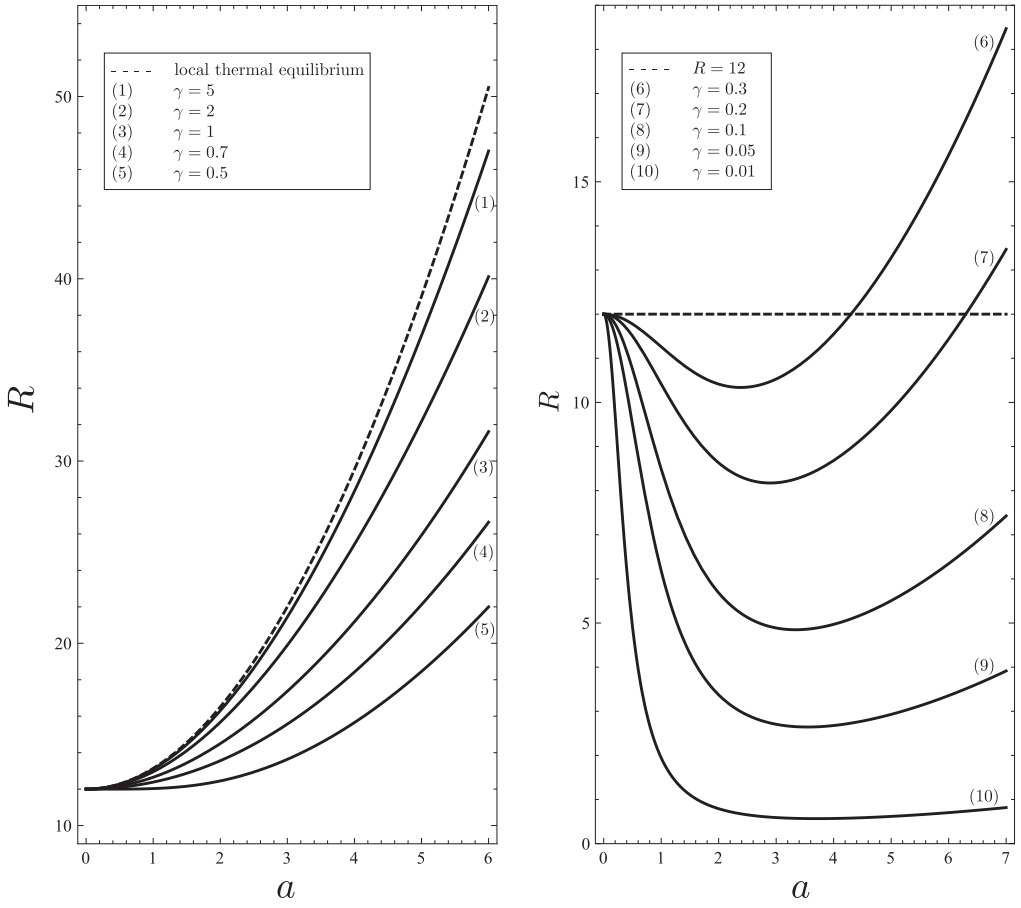

Fig. 3. Neutral stability curves for $H = 10$.

$$\widetilde{\Psi}'' - a^2\widetilde{\Psi} + aR\widetilde{\Lambda} = 0, \tag{37}$$

$$\widetilde{\Lambda}'' - a^2\widetilde{\Lambda} + a\widetilde{\Psi} = 0, \tag{38}$$

$$z = 0, 1 : \widetilde{\Psi} = 0, \quad \widetilde{\Lambda}' = 0. \tag{39}$$

We note that, on taking the limit $\gamma \to \infty$ of Eqs. (27)–(30) with a finite H, we obtain $\widetilde{\Phi} = \widetilde{\Theta}$ and

$$\widetilde{\Psi}'' - a^2\widetilde{\Psi} + aR\widetilde{\Theta} = 0, \tag{40}$$

$$\widetilde{\Theta}'' - a^2\widetilde{\Theta} + a\widetilde{\Psi} = 0, \tag{41}$$

$$z = 0, 1 : \widetilde{\Psi} = 0, \quad \widetilde{\Theta}' = 0. \tag{42}$$

By employing Eq. (31), we can conclude that the limit $\gamma \to \infty$ with a finite H yields $\widetilde{\Phi} = \widetilde{\Theta} = \widetilde{\Lambda}$. Therefore, the eigenvalue problem Eqs. (40)–(42) is completely equivalent to that given by Eqs. (37)–(39). In other words, the condition of local thermal equilibrium is attained either by taking the limit $H \to \infty$ with a finite γ, or by taking the limit $\gamma \to \infty$ with a finite H. We mention that, on account of Eq. (8), $\gamma \to \infty$ means a volumetric conductance of the fluid phase, φk_f, which is much greater than the volumetric conductance of the solid phase, $(1-\varphi)k_s$. We note that the onset criterion for Eqs. (37)–(39) or Eqs. (40)–(42) is well-known: $R_c = 12$ and $a_c = 0$; see Section 6.2 of Nield and Bejan [3].

4.2. Stationary modes with a zero wave number

Given that the local thermal equilibrium limit of the present problem has a critical wave number equal to zero and that the neutral curve has a quadratic minimum at that point, any slight relaxation of the local thermal equilibrium condition is unlikely to change this qualitative behaviour. Therefore it is a reasonable first step in our detailed analysis to consider the small-a solution.

$$(\widetilde{\Psi}, \widetilde{\Theta}, \widetilde{\Phi}, R) = (a\widetilde{\Psi}_0, \widetilde{\Theta}_0, \widetilde{\Phi}_0, R_0) + a^2(a\widetilde{\Psi}_2, \widetilde{\Theta}_2, \widetilde{\Phi}_2, R_2) + a^4(a\widetilde{\Psi}_4, \widetilde{\Theta}_4, \widetilde{\Phi}_4, R_4) + \cdots. \tag{43}$$

We substitute Eq. (43) in Eqs. (27)–(29). At $O(1)$ we obtain the equations,

$$\widetilde{\Theta}_0'' + H(\widetilde{\Phi}_0 - \widetilde{\Theta}_0) = 0, \quad \widetilde{\Phi}_0'' + H\gamma(\widetilde{\Theta}_0 - \widetilde{\Phi}_0) = 0,$$
$$\widetilde{\Psi}_0'' = -R_0\left(\frac{\gamma+1}{\gamma}\right)\widetilde{\Theta}_0. \tag{44}$$

It may be shown that these equations have the following solutions,

$$\widetilde{\Theta}_0 = \widetilde{\Phi}_0 = 1, \quad \widetilde{\Psi}_0 = -\frac{1}{2}R_0\left(\frac{\gamma+1}{\gamma}\right)(z^2 - z). \tag{45}$$

Although the common value of $\widetilde{\Theta}_0$ and $\widetilde{\Phi}_0$ should be an arbitrary constant, we have set it equal to 1 for convenience and to break the overall scale invariance of the solution. For further convenience we will set $z = \zeta + \frac{1}{2}$. As further solutions are also even about $z = \frac{1}{2}$, they will be even in ζ. Therefore the solutions given in Eq. (45) become,

$$\widetilde{\Theta}_0 = \widetilde{\Phi}_0 = 1, \quad \widetilde{\Psi}_0 = -R_0\left(\frac{\gamma+1}{\gamma}\right)\left(\frac{\zeta^2}{2} - \frac{1}{8}\right). \tag{46}$$

At $O(a^2)$ the equations for $\widetilde{\Theta}_2$ and $\widetilde{\Phi}_2$ are,

$$\widetilde{\Theta}_2'' + H(\widetilde{\Phi}_2 - \widetilde{\Theta}_2) = -\widetilde{\Psi}_0 + \widetilde{\Theta}_0, \quad \widetilde{\Phi}_2'' + H\gamma(\widetilde{\Theta}_2 - \widetilde{\Phi}_2) = \widetilde{\Phi}_0. \tag{47}$$

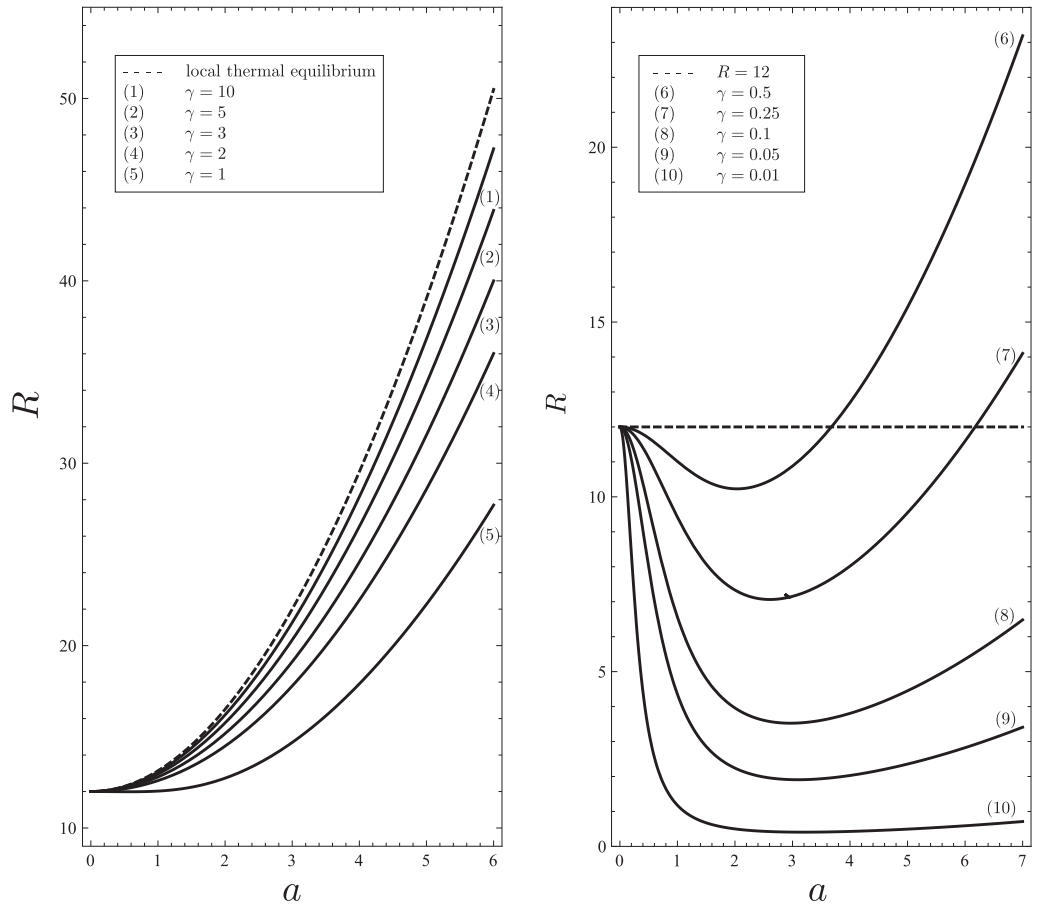

Fig. 4. Neutral stability curves for $H = 1$.

Therefore we may form,

$$\gamma\widetilde{\Theta}_2'' + \widetilde{\Phi}_2'' = (\gamma+1) + R_0(\gamma+1)\left(\frac{\zeta^2}{2} - \frac{1}{8}\right), \tag{48}$$

which may be integrated once to obtain,

$$\gamma\widetilde{\Theta}_2' + \widetilde{\Phi}_2' = (\gamma+1)\zeta + R_0(\gamma+1)\left(\frac{\zeta^3}{6} - \frac{\zeta}{8}\right), \tag{49}$$

where the constant of integration has been omitted because it is even. This quantity should be zero at the boundaries, $\zeta = \pm\frac{1}{2}$, because it is one of the boundary conditions given in Eq. (30) and this solvability condition leads to the requirement that,

$$R_0 = 12. \tag{50}$$

This result shows that the onset criterion corresponding to the zero wave number is unchanged under local thermal non-equilibrium conditions, and it is therefore independent of the values of H and γ.

Having obtained R_0 we may now complete the solution for $\widetilde{\Theta}_2$ and $\widetilde{\Phi}_2$; they are,

$$\widetilde{\Theta}_2 = B - \frac{1}{4}\zeta^2 + \frac{1}{2}\zeta^4 + \frac{12}{H^2(\gamma+1)^2\gamma}\frac{\cosh\sigma\zeta}{\cosh\frac{1}{2}\sigma} - \frac{6\zeta^2}{H(\gamma+1)\gamma}, \tag{51}$$

$$\widetilde{\Phi}_2 = B - \frac{1}{4}\zeta^2 + \frac{1}{2}\zeta^4 - \frac{12}{H^2(\gamma+1)^2}\frac{\cosh\sigma\zeta}{\cosh\frac{1}{2}\sigma} + \frac{6\zeta^2}{H(\gamma+1)} - \frac{3/2}{H\gamma} + \frac{12}{H^2(\gamma+1)\gamma}, \tag{52}$$

where $\sigma = \sqrt{H(\gamma+1)}$. The value, B, is an arbitrary constant and we may select it to be zero because its value does not affect the solvability condition at $O(a^4)$.

The equation for $\widetilde{\Psi}_2$ is now,

$$\widetilde{\Psi}_2'' = -R_0\left(\frac{\gamma+1}{\gamma}\right)\widetilde{\Theta}_2 - R_2\left(\frac{\gamma+1}{\gamma}\right)\widetilde{\Theta}_0 + \widetilde{\Psi}_0. \tag{53}$$

We omit the full expression for the right hand side of this equation for the sake of brevity, but the solution is,

$$\widetilde{\Psi}_2 = -12\left(\frac{\gamma+1}{\gamma}\right)\left[\frac{\zeta^6 - \left(\frac{1}{2}\right)^6}{60} + \frac{\zeta^4 - \left(\frac{1}{2}\right)^4}{48} - \frac{\zeta^2 - \left(\frac{1}{2}\right)^2}{16} - \frac{\zeta^4 - \left(\frac{1}{2}\right)^4}{2H(\gamma+1)\gamma} + \frac{12}{H^3(\gamma+1)^3\gamma}\left(\frac{\cosh\sigma\zeta}{\cosh\frac{1}{2}\sigma} - 1\right)\right] - R_2\left(\frac{\gamma+1}{\gamma}\right)\left(\frac{\zeta^2}{2} - \frac{1}{8}\right). \tag{54}$$

The equations for $\widetilde{\Theta}_4$ and $\widetilde{\Phi}_4$ at $O(a^4)$ are,

$$\widetilde{\Theta}_4'' + H(\widetilde{\Phi}_4 - \widetilde{\Theta}_4) = -\widetilde{\Psi}_2 + \widetilde{\Theta}_2, \quad \widetilde{\Phi}_4'' + H\gamma(\widetilde{\Theta}_4 - \widetilde{\Phi}_4) = \widetilde{\Phi}_2. \tag{55}$$

We follow the same procedure as above for $\widetilde{\Theta}_2$ and $\widetilde{\Phi}_2$, namely, we integrate once and apply the boundary condition that $\gamma\widetilde{\Theta}_4' + \widetilde{\Phi}_4' = 0$. This yields the following solvability condition,

$$R_2 = \frac{8}{7} - \frac{72}{\gamma}\left[\frac{1/5}{H(\gamma+1)} - \frac{2}{H^2(\gamma+1)^2} + \frac{24}{H^3(\gamma+1)^3} - \frac{48\tanh\frac{1}{2}\sigma}{\sigma H^3(\gamma+1)^3}\right]. \tag{56}$$

This value of R_2 is of great importance: if it is positive, then the value $a = 0$ represents a local minimum in the neutral curve. We can see from Eq. (55) that the value is $R_2 = \frac{8}{7}$ in the local thermal equilibrium limit and in that case $a = 0$ actually represents a global minimum. On the other hand, if R_2 is negative, this will imply that $a = 0$ represents a local maximum, and we should expect a global minimum at a nonzero value of a.

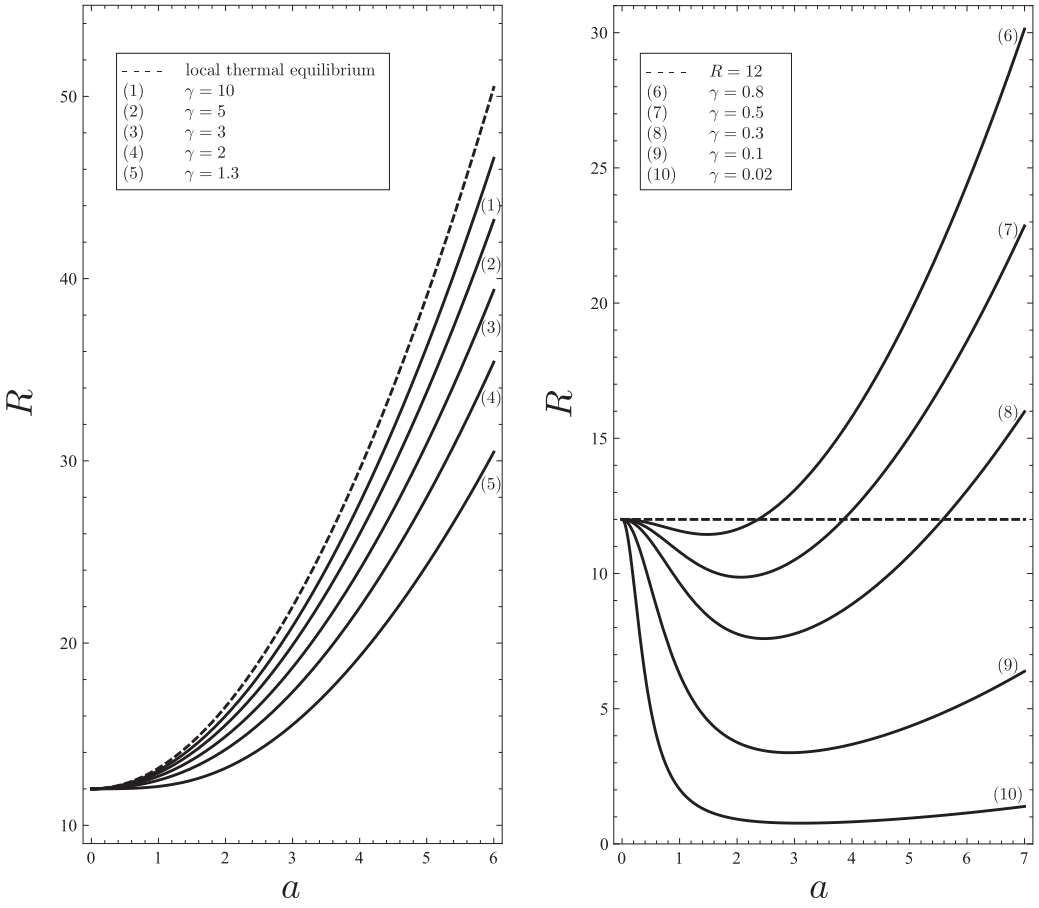

Fig. 5. Neutral stability curves for $H = 0.1$.

Anticipating our numerical results which are presented later, if we need to determine the point at which transition between $a = 0$ representing a local minimum in the neutral curve and representing a maximum, then we need $R_2 = 0$. It is not possible to determine H as an explicit function of γ or vice versa, but such threshold values of γ may be written in terms of $\sigma = \sqrt{H(\gamma+1)}$, as follows:

$$\gamma = 63\left[\frac{1}{5\sigma^2} - \frac{2}{\sigma^4} + \frac{24}{\sigma^6} - \frac{48\tanh\frac{1}{2}\sigma}{\sigma^7}\right]. \tag{57}$$

It is possible to analyse Eq. (56) further. When $H \ll 1$ then $\gamma = O(1)$ and hence $\sigma \ll 1$. The tanh function in Eq. (56) may now be expanded in a Taylor's series and we obtain,

$$R_2 = \frac{8}{7} - \frac{72}{\gamma}\left[\frac{17}{840} + O(H)\right] \tag{58}$$

Therefore $R_2 = 0$ when

$$\gamma = \frac{51}{40} + O(H). \tag{59}$$

On the other hand, when $H \to \infty$ and $\gamma \to 0$, then it is clear that $\sigma \to \infty$. Therefore Eq. (56) becomes,

$$R_2 \sim \frac{8}{7} - \frac{72}{5H\gamma} \tag{60}$$

at leading order. Hence $R_2 = 0$ implies that

$$H\gamma = \frac{63}{5}. \tag{61}$$

4.3. Numerical solution

The eigenvalue problem Eqs. (32)–(35) can be solved numerically by employing a sixth-order Runge–Kutta solver combined with a shooting technique. More precisely, Eqs. (32)–(34) can be integrated numerically by means of the Runge–Kutta solver with the initial conditions

$$\begin{aligned} &\widetilde{\Psi}(0) = 0, \quad \widetilde{\Psi}'(0) = \eta, \quad \widetilde{\Lambda}(0) = 1, \quad \widetilde{\Lambda}'(0) = 0, \\ &\widetilde{\Phi}(0) = \frac{\gamma}{1+\gamma}, \quad \widetilde{\Phi}'(0) = \xi. \end{aligned} \tag{62}$$

As already noted in Section 4.2, the condition $\widetilde{\Lambda}(0) = 1$ serves to break the overall scale invariance of the solution. On the other hand, the parameters η and ξ, that denote the values of $\widetilde{\Psi}'(0)$ and $\widetilde{\Phi}'(0)$ respectively, are unknown and are determined, together with the eigenvalue R, by imposing the three boundary conditions at $z = 1$,

$$\widetilde{\Psi}(1) = 0, \quad \widetilde{\Lambda}'(1) = 0, \quad \widetilde{\Phi}(1) = \frac{\gamma}{1+\gamma}\widetilde{\Lambda}(1). \tag{63}$$

The parameters η, ξ and R can be solved for by satisfying the constraints defined by Eq. (63) through the shooting method.

The numerical procedure is implemented in the *Mathematica 8* (© Wolfram Research, Inc.) environment [19]. The Runge–Kutta solver is available through the built-in function `NDSolve` by setting the option

```
Method->{"ExplicitRungeKutta", "DifferenceOrder"->6}
```

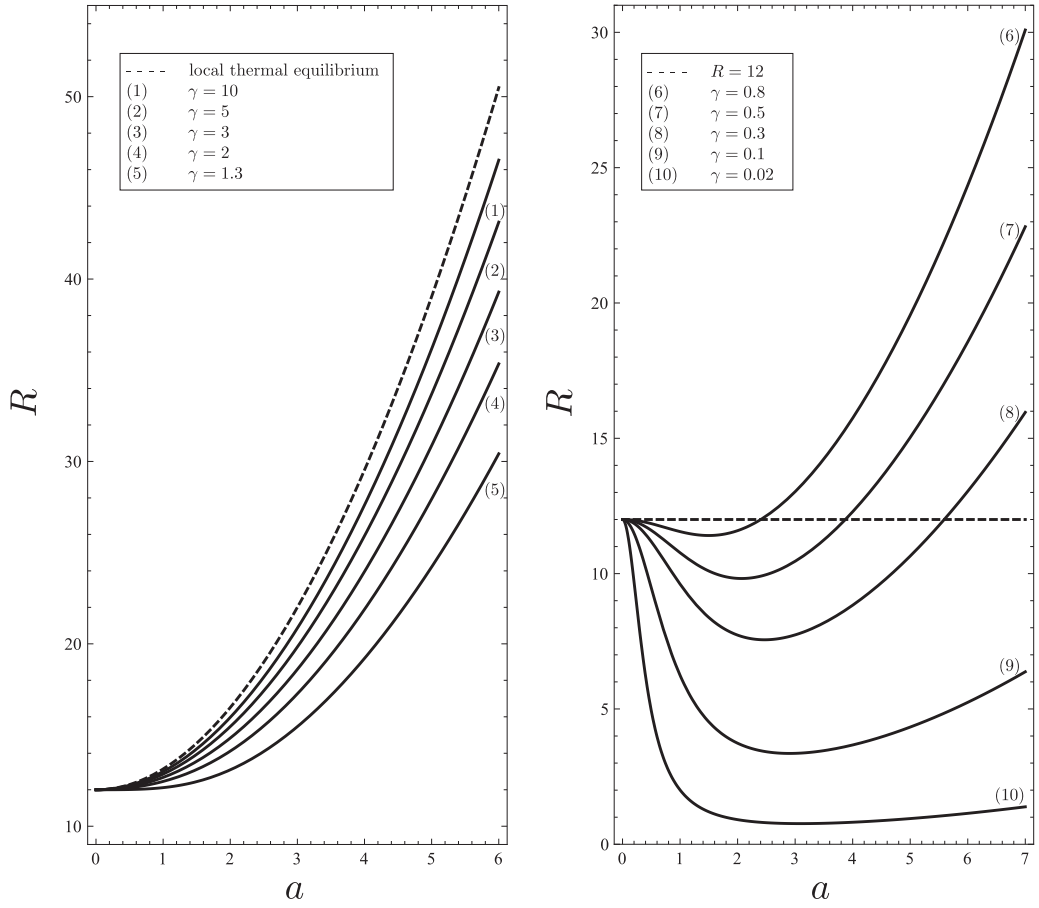

Fig. 6. Neutral stability curves in the limit $H \to 0$.

The shooting method is implemented by the built-in function `FindRoot` that allows one to solve numerically the constraints Eq. (63). The overall numerical procedure requires the assignment of the input data (a,H,γ). Thus, we obtain a neutral stability curve $R(a)$ for every pair (H,γ). The absolute minimum of $R(a)$ is for the critical values (a_c,R_c).

5. Discussion of the results

5.1. Neutral stability

Neutral stability curves in the (a,R)-plane are displayed in Figs. 2–6, for $H = 100$, 10, 1, 0.1, and in the limit $H \to 0$ respectively. For a fixed H, the neutral stability curves correspond to different values of γ. In Figs. 2–6, the left hand frame is for the higher values of γ, and the dashed line is the neutral stability curve for the local thermal equilibrium (either $H \to \infty$ or $\gamma \to \infty$). As shown in Section 4.1.1, for the case of local thermal equilibrium, the neutral stability condition is independent of γ. The right hand frames of Figs. 2–6, are for the lower values of γ, and the dashed line denotes the horizontal line $R = 12$. These figures clearly show that, in every case, the limit of R for $a \to 0$ is 12, as proved analytically in Section 4.2. However, the shape of the neutral stability curves displays a strong dependence on γ. These figures show that, for a prescribed H, the neutral stability function $R(a)$ displays the monotonic increasing trend typical of the local thermal equilibrium only if γ is sufficiently high. If γ drops below a threshold value, which is dependent on H and which is given by Eq. (57), then the monotonically increasing behaviour of the neutral curve is lost and R decreases with a at first, reaches a minimum, and then starts increasing. Stated differently, for a prescribed H, there exists a threshold value of γ, denoted as γ_{th}, such that the critical value of R is $R_c = 12$, with $a_c = 0$, when $\gamma > \gamma_{th}$. On the contrary, when $\gamma < \gamma_{th}$, the critical value of R is smaller than 12 and the critical wave number is nonzero. Values of γ_{th} are reported in Table 1 versus H. This table shows that γ_{th} is a monotonically decreasing function of H that ranges from 0, in the limit $H \to \infty$, to 1.27500 = 51/40, in the limit $H \to 0$. This is confirmed in Fig. 7 which shows the variation of the threshold value of γ against H as calculated from Eq. (57). Also shown are the large and small-H asymptotic behaviours, as given by Eqs. (59) and (61).

Table 1
Values of γ_{th}.

H	γ_{th}
∞	0
500	0.0241359
100	0.104646
50	0.182481
10	0.505054
5	0.687453
1	1.05528
0.5	1.14979
0.1	1.24663
0.05	1.26057
0.01	1.27207
0	1.27500

It is worth noting that Figs. 2–5 illustrate how, for large values of γ, the local thermal equilibrium is approached either for small or large values of H. This feature is consistent with what has been pointed out in Section 4.1.1 with respect to the limit $\gamma \to \infty$ for a

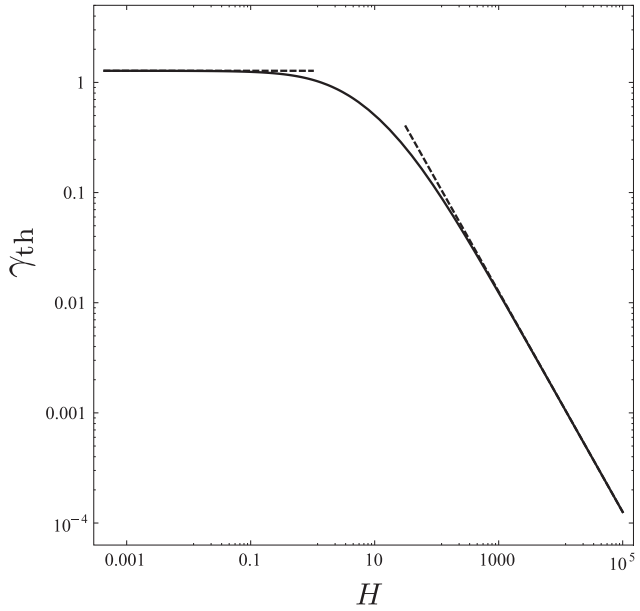

Fig. 7. Variation of $\gamma_{\rm th}$ with H as given by Eq. (57). Also shown are the large and small-H asymptotic behaviours, as given by Eqs. (59) and (61).

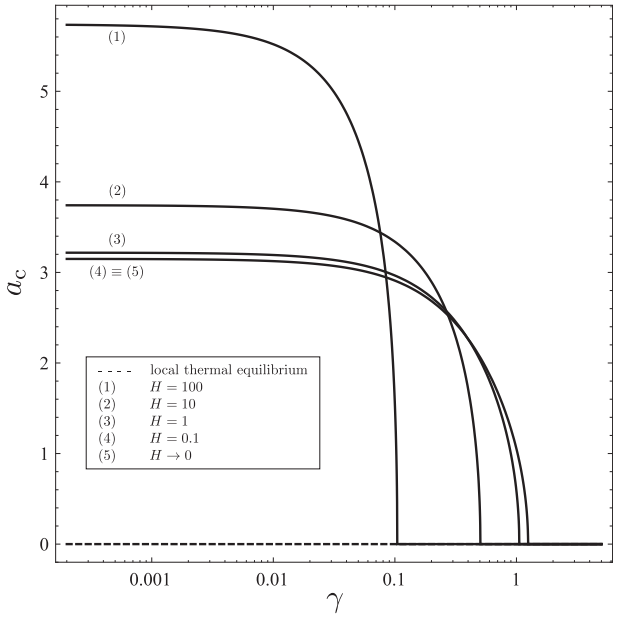

Fig. 9. Plots of $a_{\rm c}$ versus γ for assigned values of H.

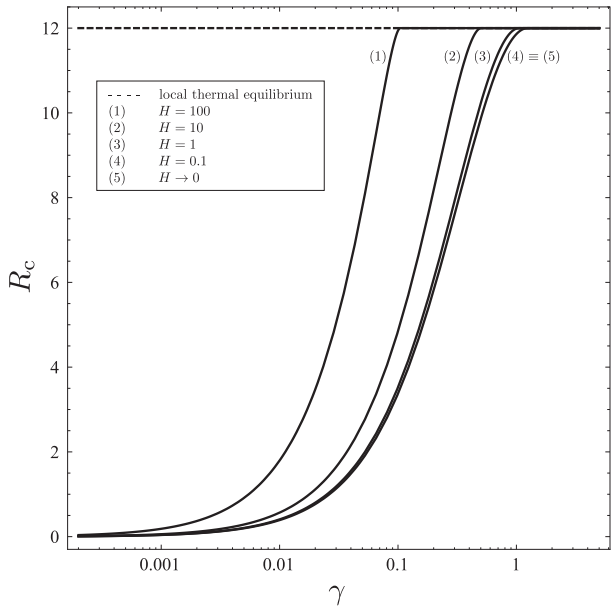

Fig. 8. Plots of $R_{\rm c}$ versus γ for assigned values of H.

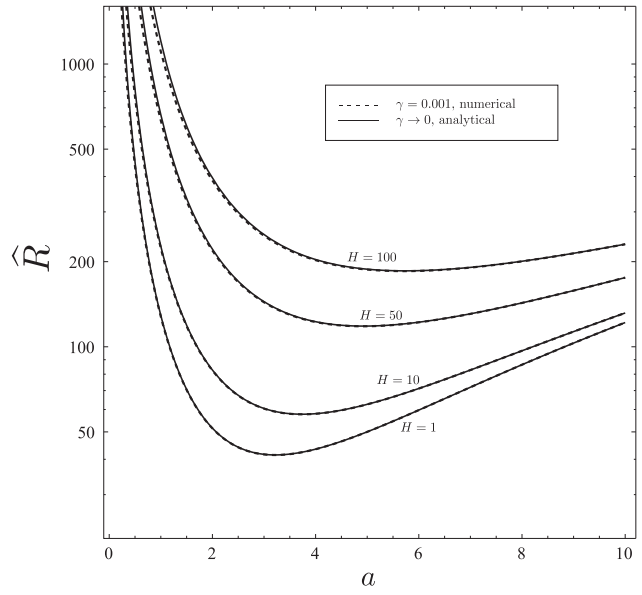

Fig. 10. Neutral stability curves, $\widehat{R}$ versus a, for $\gamma \ll 1$ and different values of H: comparison between the numerical solution with $\gamma = 0.001$ (dashed lines) and the analytical solution, Eq. (73), in the limit $\gamma \to 0$ (continuous lines).

finite H. We mention that the limiting case $H \to 0$, illustrated in Fig. 6, corresponds to a regime where there is no heat transfer between the solid and the fluid phase. This regime is the condition farthest from the local thermal equilibrium. However, Fig. 6 shows that the departure of the neutral stability curve from that of local thermal equilibrium is not so marked, provided that γ is sufficiently high, say $\gamma > 10$. A comparison between Figs. 5 and 6 shows that the neutral stability curves with $H = 0.1$ and with $H \to 0$ display only very slight differences, thus showing that with $H = 0.1$ we attain a condition very close to the complete thermal decoupling between the phases, i.e. to the limiting case $H \to 0$.

Plots of $R_{\rm c}$ against γ and $a_{\rm c}$ against γ are displayed in Figs. 8 and 9 for different values of H. These figures show clearly that the critical conditions for the onset of the instability are the same as for local thermal equilibrium, i.e. $a_{\rm c} = 0$ and $R_{\rm c} = 12$, when $\gamma > \gamma_{\rm th}$. For lower values of γ, we gather from these figures that $R_{\rm c}$ is an increasing function of γ, while $a_{\rm c}$ is a decreasing function of γ. In particular, we expect from Fig. 8 that $R_{\rm c} \to 0$ when $\gamma \to 0$, for every value of H.

5.2. The limiting case $\gamma \to 0$

Physically, the limit $\gamma \to 0$ means a condition where the solid phase is much more conducting than the fluid phase, on assuming that the porosity is kept fixed.

The eigenvalue problem Eqs. (27)–(30) can be formulated so

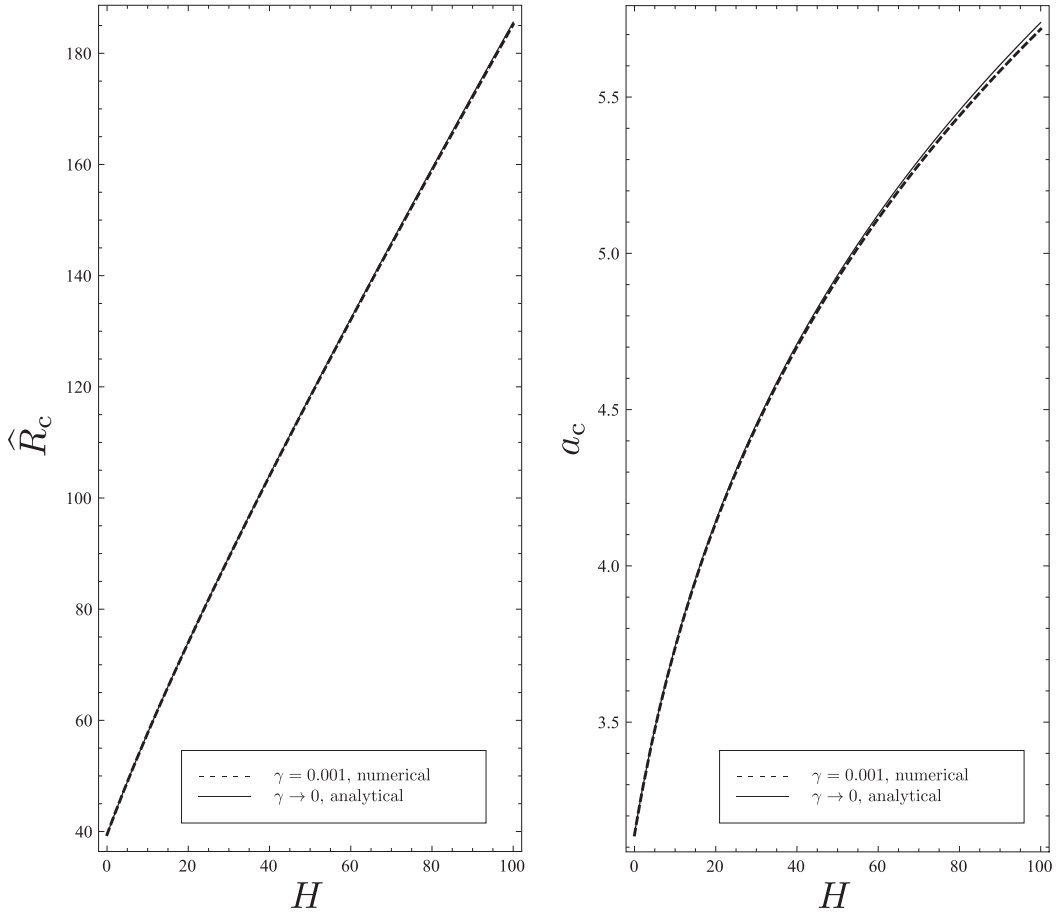

Fig. 11. Plots of $\widehat{R}_c$ versus H (left hand frame) and of a_c versus H (right hand frame), for $\gamma \ll 1$: comparison between the numerical solution with $\gamma = 0.001$ (dashed lines) and the analytical solution, Eq. (74), in the limit $\gamma \to 0$ (continuous lines).

that it is well-posed when $\gamma \to 0$. We define the modified Darcy–Rayleigh number as

$$\widehat{R} = \frac{1+\gamma}{\gamma} R. \tag{64}$$

Then, on taking $\gamma \to 0$ with a finite $\widehat{R}$, Eqs. (27)–(30) yield

$$\widetilde{\Psi}'' - a^2 \widetilde{\Psi} + a\widehat{R}\widetilde{\Theta} = 0, \tag{65}$$

$$\widetilde{\Phi}'' - a^2 \widetilde{\Phi} = 0, \tag{66}$$

$$\widetilde{\Theta}'' - a^2 \widetilde{\Theta} + H(\widetilde{\Phi} - \widetilde{\Theta}) + a\widetilde{\Psi} = 0, \tag{67}$$

$$z = 0, 1 : \widetilde{\Psi} = 0, \quad \widetilde{\Phi}' = 0, \quad \widetilde{\Theta} = \widetilde{\Phi}. \tag{68}$$

Eq. (66) with the boundary conditions on Φ expressed by Eq. (68) admits, for an arbitrary a, the unique solution $\Phi = 0$. Then the system Eqs. (65)–(68) can be reduced to

$$\widetilde{\Psi}'' - a^2 \widetilde{\Psi} + a\widehat{R}\widetilde{\Theta} = 0, \tag{69}$$

$$\widetilde{\Theta}'' - (a^2 + H)\widetilde{\Theta} + a\widetilde{\Psi} = 0, \tag{70}$$

$$z = 0, 1 : \widetilde{\Psi} = 0, \quad \widetilde{\Theta} = 0. \tag{71}$$

Eqs. (69)–(71) can be solved analytically with

$$\Psi(z) = \sin(\pi z), \quad \Theta(z) = A \sin(\pi z), \tag{72}$$

where A is an integration constant. We obtain

$$\widehat{R} = \frac{(\pi^2 + a^2)(\pi^2 + a^2 + H)}{a^2}. \tag{73}$$

By seeking the minimum of $\widehat{R}$ versus a, we get the critical values

$$a_c = \sqrt{\pi}(H + \pi^2)^{1/4}, \quad \widehat{R}_c = H + 2\pi(\pi + \sqrt{H + \pi^2}). \tag{74}$$

Interestingly enough, Eq. (74) yields the well-known critical values $a_c = \pi$ and $\widehat{R}_c = 4\pi^2$, when $H \to 0$. These values are those obtained for the Darcy–Bénard problem with Dirichlet boundary conditions under the assumption of local thermal equilibrium [3].

Eqs. (73) and (74), together with Eq. (64), provide a useful approximate solution to be employed when $\gamma \ll 1$. In particular one may justify rigorously, on the basis of Eqs. (64) and (74), that $R_c \to 0$ with $\gamma \to 0$ for every value of H, i.e. the behaviour guessed when we commented on Fig. 8.

Fig. 10 displays the neutral stability curves, $\widehat{R}(a)$, with $\gamma \ll 1$ and different values of H. The continuous lines are for the limiting case $\gamma \to 0$, and have been obtained by the analytical solution Eq. (73). The dashed lines are for $\gamma = 0.001$, and have been obtained by the numerical solution described in Section 4.3. The agreement is definitely satisfactory and represents an argument to assess that Eq. (73) can be safely employed when γ is small, both for small and for large values of H. We see that the agreement between the results for $\gamma = 0.001$ and $\gamma \to 0$ is almost perfect when H is small while, for larger values of H, there is a slight discrepancy with smaller wave numbers.

The comparison between the numerical and the analytical solutions for $\gamma = 0.001$ and $\gamma \to 0$, respectively, is displayed also in Fig. 11, where the critical values $\widehat{R}_c$ and a_c are plotted versus H.

Again, we conclude that the agreement is very good, except for a slight discrepancy in the plots of a_c versus H when H is approximately greater than 80.

6. Conclusions

The onset of convection in a plane horizontal porous layer subjected to a uniform upward heat flux has been investigated. We have considered cases where local thermal non-equilibrium exists between the solid and the fluid phases as modelled by an inter-phase heat transfer coefficient. The stationary basic solution has a zero velocity field, and displays local thermal equilibrium between the phases, with a linear temperature distribution in the vertical direction.

We studied the linear stability of the basic state by solving the momentum and energy disturbance equations formulated in terms of a streamfunction, and of the temperature perturbations of the solid and fluid phases. The disturbance equations for the normal modes produced a system of three ordinary differential equations. The governing parameters are (R,H,γ), namely the Darcy–Rayleigh number, the inter-phase heat transfer parameter, and the conductivity ratio between the phases, as well as the wave number a of the normal mode. We solved numerically this system of ODEs as an eigenvalue problem, for prescribed values of (H,γ).

The numerical solution, carried out by the Runge–Kutta method and by the shooting method, yields R as a function of a along the neutral stability curve and, on seeking the minimum of this curve, the critical values (a_c,R_c). The limiting case $H \to \infty$ has been studied for the regime of local thermal equilibrium. We proved that the same solution is obtained on keeping H finite and letting $\gamma \to \infty$. The latter limit means a fluid phase much more conductive than the solid phase. The opposite limit, $\gamma \to 0$, has been investigated as well, and an analytical solution was found in this special case.

We proved analytically that the limiting value of $R(a)$ at neutral stability when $a \to 0$ is 12, for every choice of (H,γ). Nield [14] pointed out that $R \to 12$ when $a \to 0$ under conditions of local thermal equilibrium, for a porous layer with Neumann boundary conditions on the temperature field. We demonstrated that Nield's result holds also when the assumption of local thermal equilibrium is relaxed. In the case of local thermal equilibrium, $R = 12$ is the critical value, since the neutral stability curve $R(a)$ is monotonically increasing. When local thermal non-equilibrium conditions prevail, this behaviour is observed only when γ is larger than a threshold value which depends on H. If γ is smaller than the threshold value then $R_c < 12$ and $a_c > 0$.

The general behaviour is that the local thermal non-equilibrium has a destabilising effect; a behaviour already observed for the case of Dirichlet thermal boundary conditions by Banu and Rees [9].

The uniform heat flux condition at the boundaries has been formulated here by adopting the so-called Model A [15]. This model is based on the energy balance at the boundary of the porous medium, and on the assumption that the solid phase and the fluid phase temperatures coincide on the boundary, $\overline{T}_s = \overline{T}_f$. Without this additional condition the problem would have been underdetermined. The boundary condition $\overline{T}_s = \overline{T}_f$ is justified as far as the boundary walls are highly conducting, but it is not clear which condition should be used otherwise. We mention that several possibilities have been stated by different authors, and a comparison between them was carried out by Alazmi and Vafai [20]. We cannot make an *a priori* assessment of what might happen if Model A is replaced by another model of the uniform heat flux boundary conditions. But it is certain that even the basic solution is affected by an altered form of the uniform heat flux condition at the boundaries. These authors think that deeper insights into this aspect of the stability problem investigated here may be an interesting opportunity for future research.

References

[1] C.W. Horton, F.T. Rogers, Convection currents in a porous medium, J. Appl. Phys. 16 (1945) 367–370.
[2] E.R. Lapwood, Convection of a fluid in a porous medium, Proc. Cambridge Phil. Soc. 44 (1948) 508–521.
[3] D.A. Nield, A. Bejan, Convection in Porous Media, 3rd ed., Springer, New York, 2006.
[4] A. Anzelius, Über Erwärmung vermittels durchströmender Medien, Z. Angew. Math. Mech. 6 (1926) 291–294.
[5] T.E.W. Schumann, Heat transfer: A liquid flowing through a porous prism, J. Franklin Inst. 208 (1929) 405–416.
[6] M. Combarnous, S. Bories, Modelisation de la convection naturelle au sein d'une couche poreuse horizontale a l'aide d'un coefficient de transfert solide–fluide, Int. J. Heat Mass Transf. 17 (1974) 505–515.
[7] A.V. Kuznetsov, Thermal nonequilibrium forced convection in porous media, in: D.B. Ingham, I. Pop (Eds.), Transport Phenomena in Porous Media, Pergamon, Oxford, 1998, pp. 103–129.
[8] D.A.S. Rees, I. Pop, Local thermal non-equilibrium in porous medium convection, in: D.B. Ingham, I. Pop (Eds.), Transport Phenomena in Porous Media III, Pergamon, Oxford, 2005, pp. 147–173.
[9] N. Banu, D.A.S. Rees, Onset of Darcy–Bénard convection using a thermal non-equilibrium model, Int. J. Heat Mass Transf. 45 (2002) 2221–2228.
[10] A. Postelnicu, D.A.S. Rees, The onset of Darcy–Brinkman convection in a porous layer using a thermal nonequlibrium model – Part I: stress-free boundaries, Int. J. Energy Res. 27 (2003) 961–973.
[11] A. Postelnicu, The onset of a Darcy–Brinkman convection using a thermal non-equilibrium model. Part II, Int. J. Thermal Sci. 47 (2008) 1587–1594.
[12] M.S. Malashetty, I.S. Shivakumara, S. Kulkarni, The onset of convection in an anisotropic porous layer using a thermal non-equilibrium model, Trans. Porous Media 60 (2005) 199–215.
[13] A. Nouri-Borujerdi, A.R. Noghrehabadi, D.A.S. Rees, Onset of convection in a horizontal porous channel with uniform heat generation using a thermal non-equilibrium model, Trans. Porous Media 69 (2007) 343–357.
[14] D.A. Nield, Onset of thermohaline convection in a porous medium, Water Resour. Res. 4 (1968) 553–560.
[15] A. Amiri, K. Vafai, T.M. Kuzay, Effect of boundary conditions on non-Darcian heat transfer through porous media and experimental comparisons, Numer. Heat Transf. A 27 (1995) 651–664.
[16] K. Yang, K. Vafai, Analysis of temperature gradient bifurcation in porous media – An exact solution, Int. J. Heat Mass Transf. 53 (2010) 4316–4325.
[17] J. Bear, Dynamics of Fluids in Porous Media, Dover, New York, 1988.
[18] D.A. Nield, Modeling the effects of a magnetic field or rotation on flow in a porous medium: momentum equation and anisotropic permeability analogy, Int. J. Heat Mass Transf. 42 (1999) 3715–3718.
[19] S. Wolfram, The Mathematica Book, 5th ed., Wolfram Media, Champaign, IL, 2003.
[20] B. Alazmi, K. Vafai, Constant wall heat flux boundary conditions in porous media under local thermal non-equilibrium conditions, Int. J. Heat Mass Transf. 45 (2002) 3071–3087.